Cross-stream Active Mooring for Tidal Stream Power Systems

Che-Chih Tsao[#1], Jia-Shi Lee[#], Yen-Yu Chen[#], Yu-Sheng Chen[#], Yi-Feng Hsu[#]

[#]*Department of Power Mechanical Engineering, National Tsing Hua University*
101 Kuang-fu Rd. Sec. 2, Hsinchu, Taiwan, Republic of China

[1]cctsao@pme.nthu.edu.tw

***Abstract*— A new design for mooring tidal stream turbines is proposed and its feasibility is studied by analysis and scaled model tests. The design features mooring multiple turbines on a common tether with anchoring only at two ends. The whole array of turbines is in submerged floating with only two major lifting buoys partially above water surface. A new method to moor a single turbine on the common tether was devised and tested using models. The mooring system can prevent the single turbine from rolling and also allow bi-directional operation by a vertical flipping motion. An end clump system was also designed to work with the new turbine mooring method and the lifting buoys to maintain the turbines within desired depth range in varying operating flow speeds. Analysis in mechanics provided example designs and corresponding parameters. Scaled model tests demonstrated the feasibility of the single turbine mooring method and the end clump depth maintaining approach.**

***Keywords*— tidal streams, mooring, marine current, power generation, turbine array**

I. INTRODUCTION

Tidal stream power are stable, predictable and can be found in many locations. In addition, compared to other approaches for harnessing ocean tidal power, tidal stream power systems may have the least impacts on environments.[1] Currently, there are many on-going efforts in developing practical tidal stream power systems. Typical examples include systems from the Atlantic Resources (e.g. the SeaGen featuring horizontal axis turbine fixed to seafloor) [2], the Open Hydro (tube turbine placed on seafloor) [3], the Scotrenewables (e.g. SR2000 floating system) [4], the Blue Energy Services (the BlueTEC floating single turbine) [5] and the Blackrock Tidal / Schottel (semi-submerged system) [6]. There are also examples from the OIST (floating single turbine) [7] and the IHI Engineering (submerged floating twin turbines) [8].

Pilot plants of some of the above systems have been constructed and some of them have already been connected to local grid to start generating power. However, the supporting/mooring methods used by the above systems still have issues that may hinder their installations in large scale due to cost-effectiveness.

First, systems fixed to or placed on seafloor requires larger hub elevation in waters of larger depth in order to access faster flow closer to sea surface, which may not be cost-effective.

Second, individual installation or mooring of each turbine unit on seafloor is associated with high construction cost and environmental impacts.

Further, floating systems are disadvantageous to other usages of water surface, although they have cost advantage over fixed systems in waters of significant depth.

Still further, individually moored floating or submerged floating systems must be placed with enough spacing among adjacent systems to avoid interference in variant flows. This spacing becomes larger in areas of deeper waters, because longer mooring lines must be used, which could reduce efficiency of area usage, given that the area of fast streams in a tidal flow zone is limited.

Another issue involves natural variations of flow patterns. It has been shown that turbines in a multi-row formation should be arranged in staggered positions to minimize wake effects [9-10]. Due to winds and other effects such as non-tidal currents, directions of tidal flows may sway frequently. Examples can be seen in Penghu Channel west of Taiwan [11-13]. Systems fixed to or placed on seafloor cannot accommodate such variations and the overall efficiency of the formation could suffer. Even more serious, in some locations, core passages of flood flow and of ebb flow deviate significantly, posing problems to bidirectional operations. Such cases can be found, for examples, in Inner Sound of Pentland Firth, Scotland [14], Goto Islands of Kyushu, Japan [15], and Zhoushan of Zhejiang, China [16].

Still another issue concerns balancing of turbine torque and ease of bi-directional operation. When applying a floating or submerged floating system to support a turbine, torque created by the turbine's rotor needs to be balanced. A typical approach is using a twin-turbine unit, connecting two counter-rotating turbines into a rigid unit and let the two torques cancel each other [4, 8, 17]. However, because flows are turbulent and rarely uniform, not only torques but also thrusts can become uneven and result in yawing and rolling instability [17]. Therefore, additional stabilizing means, such as rotor speeds controlling, hydrodynamic control surfaces and hydraulic pose balancing, may be necessary. Furthermore, torques' effects on the internal structure of the unit cannot be reduced. The structure must have enough material in order to resist the associated internal stress, which also increases complexity and costs.

Another approach capable of supporting a single turbine applies a vertical structure with a buoy (or a floating body) at top and a ballast (or the turbine itself) at bottom for torque balancing [5, 7]. However, when turning with flow this configuration must turn about a vertical axis. Therefore, it may need an auxiliary mechanism to make sure that mooring

lines and power takeoff cables are not over twisted in repeated bi-directional operations.

The Cross-stream Active Mooring (CSAM) is a concept recently proposed by the authors for mooring generator turbines in arrays in an ocean current over deep seafloor. Large formations of turbines can be deployed from concentrated small anchoring footprints, potentially saving significant undersea construction costs and making minimal impact to the seafloor. Improved gravity anchors are used to anchor tethers of the arrays on shallow locations, such as on tops of undersea ridges and a submerged hydro sail system close to the generator turbines acts as "active anchors" to deploy the arrays of turbines transversely across current streams and hold the systems in position over deep sea. Further, the hydro sail system can adjust the position of the system arrays to track current meanders and place turbines always within fast streams in the current velocity core.[18-20] The CSAM concept, with proper adjustments, can also be applied to scenarios in tidal streams.

This work proposes a new mooring design for tidal stream power based on the CSAM concept with the features of mooring by linear arrays, submerged floating systems and capability of array lateral displacement for the purpose of construction cost savings, environmental considerations and increasing power capturing efficacy.

II. Basic Concept

Figure 1 illustrates the basic configuration of the proposed "Tidal CSAM" system. The features of the design concept and their design goals are described as follows:

A. Mooring turbines on a common tether

Multiple turbine units (TU) are moored onto a common tether (called array tether TA), instead of on seafloor, to form a linear array of generators. The two ends of the array tether are connected to two main mooring tethers respectively. The two main mooring tethers (called head tether TM_{head} and tail tether TM_{tail}) are then anchored to seafloor at two anchors (called head anchor AN_{head} and tail ancho AN_{tail}) respectively. (For convenience, the direction toward the flooding tide is called head and the opposite direction tail.)

This design requires only very limited marine construction works, reducing installation costs and minimizing environmental impacts. Further, because turbines are moored to the array tether with relatively short mooring lines, turbines in the same array can be placed closely without the risk of mechanical interference.

B. Submerged floating turbines

Most part of the tidal CSAM system is kept in submerged floating under sea surface. Each turbine unit is built with extra buoyancy so that it floats upwards. But all turbine units in the array, their mooring lines, their anchors on the array tether and the array tether as a whole are kept at near neutral buoyancy. At both ends (head and tail), the end section of the array tether (TA_{eh} or TA_{et}) connects first to an end clump (head clump CLP_{head} or tail clump CLP_{tail}) and then, through a hanging section of tether (TA_{hh} or TA_{ht}), to a lifting buoy (LB_{head} or LB_{head}). The two end clumps provide extra weight over the near-neutral buoyancy turbine array and pulls the whole array downwards. The lifting buoys, moored by mooring tethers toward the head direction and the tail direction, are semi-submerged and provide extra buoyancy to counter the downward pulls from the end clumps. As a result, the whole system is kept floating by the two lifting buoys but the array of turbines is kept in submerged floating.

By proper design, to be discussed later, the array tether can be maintained within a prescribed depth range regardless of depth of seafloor. In this way, most sea surface areas can still be utilized.

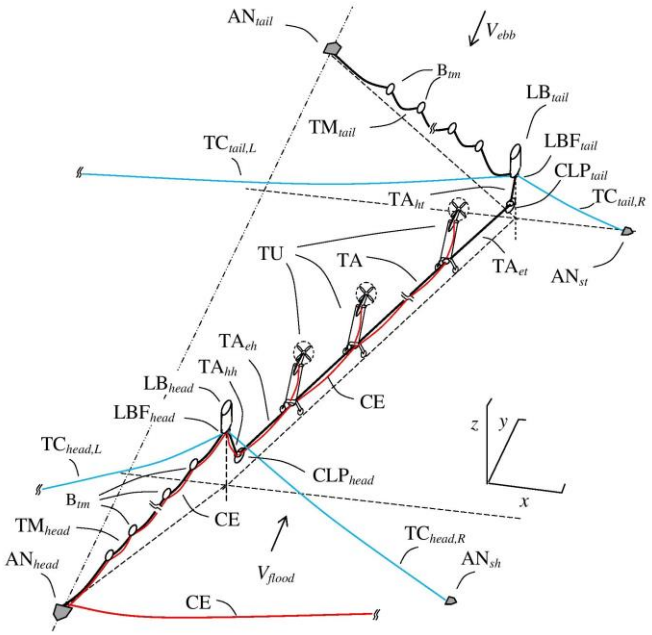

Fig. 1 Basic concept of the Tidal CSAM system. See texts for symbols.

C. Single turbine mooring, torque balancing, bi-directional operations

Although the design features described above can be applied to various forms of marine turbine unit, an unit of a single horizontal axis turbine could be the most cost effective choice. Among various types of fluid kinetic power convertor, horizontal axis turbines have been shown to be the most efficient by the wind power industries [21]. A single turbine of simple construction with minimal external structure will have the lowest unit cost.

A new turbine mooring system is devised to moor a single turbine on the horizontal array tether and at the same time balance turbine torque, while also being capable of bi-directional operations by turning with tidal flows by flipping along a vertical path (i.e. about a horizontal axis).

Figure 2(a) shows the new mooring system with the turbine in operational pose. The turbine unit takes the form of a long nacelle and a downstream rotor. Two mooring lines (left and right) moor the turbine at two mooring handles on the nacelle to a mooring base on the array tether. A spacing is maintained between the two mooring lines by the handles and the base.

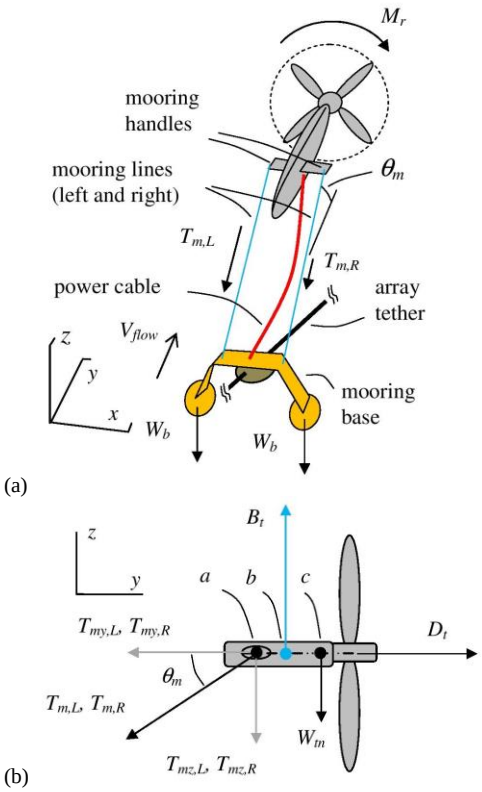

Fig. 2 (a) The single turbine mooring system with a turbine in its operational pose; (b) force analysis of the turbine in side view.

The turbine is built with extra buoyancy so that it floats above the depth of the array tether and the mooring lines form an angle (θ_m) with respect to the horizon. The extra buoyancy and thrust on the rotor create tensions on the two mooring lines. The torque (M_r) exerted by the rotor to the nacelle makes the nacelle to roll and the mooring base also rolls. The mooring base comprises a seagull shaped frame with two ballast weights (W_b) at two ends below the level of the array tether. As the mooring base rolls, one ballast weight moves up and the other down, creating a countering torque to the rotor torque. As a result, the tension on the left mooring line ($T_{m,L}$) is larger than that on the right mooring line ($T_{m,R}$) and this tension difference acts on the mooring handles to counter the turbine torque and prevent the turbine from over-rolling. .

Figure 2(b) depicts the turbine in its horizontal operational pose in side view with force vectors. To keep the turbine nacelle at horizontal pose during operation, the positions of the buoyancy center (b) and mass center of the turbine (c) with respect to the fairleads (a) need to be arranged as depicted in the figure so that the moment of buoyancy force cancels the moment of weight, while thrust on the downstream rotor keeps the nacelle in near-horizontal pose along the flow.

The moment of buoyancy force with respect to the fairleads is further made slightly larger than the moment of weight and the fairleads on the torque handles are placed in the same line as the buoyancy center and the mass center but to their upstream direction, so that in low or no flow conditions the extra moment will rotate the turbine up to a vertical pose. When the tidal stream reverses direction the turbine leans toward the reversed direction, passing across the array tether, and takes a horizontal operational pose again. Figure 3 illustrates the scenarios.

This arrangement can simplify configuration of the turbine. A rotor with fixed pitch blades or a passive pitch adjustment mechanism can be used. The turbine turns with tidal flows by flipping along a vertical path, with no need of slip joint nor risk of over-twisting either the mooring lines or power cable.

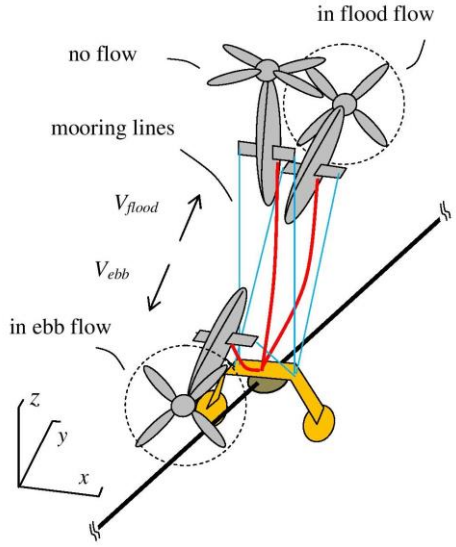

Fig. 3 Bi-directional operations of the single turbine mooring system

D. Array depth keeping

The submerged floating turbines should be kept within a preferred depth range in most operating conditions. However, the vertical distance between the turbine and the array tether changes when the flow speed changes and when the turbine flips with tidal flows along the vertical path. Different flow speeds also result in varying total pulling force at the fairleads of the lifting buoys (LBF_{head} or LBF_{tail}), which could change their depths. The end clumps (CLP_{head}, CLP_{tail}) and the hanging sections of the array tether (TA_{hh}, TA_{ht}) are designed to compensate for these variations. Figure 4(a) shows a side view of the end clump depth keeping system. In fast flows, the turbines sink down by increased thrusts. But increased thrusts on the whole turbine array also increase the pull on the end clump and raise the whole array up. By matching the designs of the mooring system of the turbine unit, the end clump systems and the lifting buoys, the turbines can be kept within a preferred depth range (d_{TU}) in most conditions.

E. Cross-stream deployment of turbine array

By placing and mooring the two lifting buoys at the two ends of the array across the track of tidal streams, the turbine array can be deployed across the tidal stream so that downstream turbines are not blocked by upstream turbines.

The whole turbine array including the mooring tethers is anchored at two ends. When the tide floods, the whole array pulls on the head anchor; when the tide ebbs, the tail anchor takes loads.

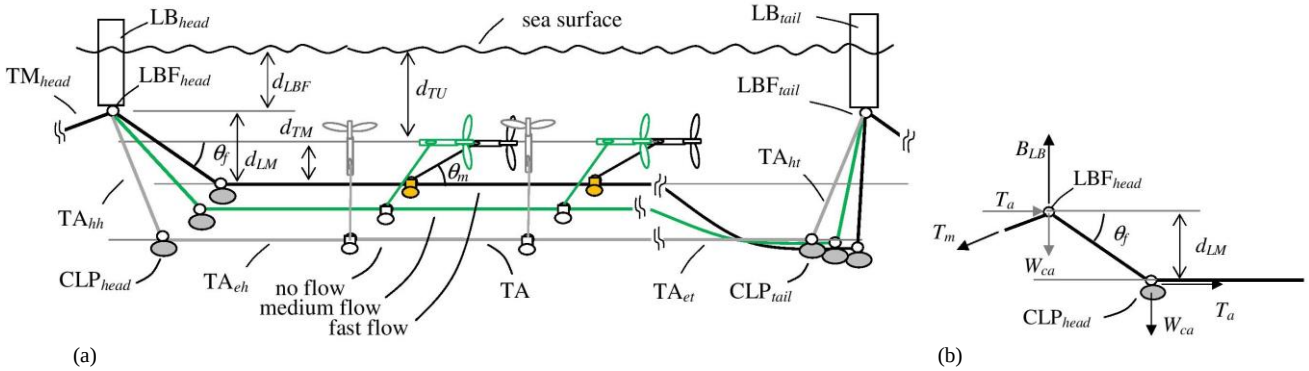

Fig. 4(a) The end clump depth keeping system in side view; (b) force analysis.

F. 2D formation of multiple turbine arrays

When a second array of turbines is added, proper spacing from behind the first array can be taken and turbines can be placed in staggered positions with respect to the first array to minimize wake effect. Thus, multiple linear arrays of turbines can be deployed to form a 2D formation.

G. Active positioning of turbines

Since the whole turbine array is kept floating by the two lifting buoys and is anchored through mooring tethers only at two anchoring points, position and angle of deployment of the turbine array can be adjusted by adjusting positions of the two lifting buoys. This can be done by applying a set of winched lateral control lines (TC$_{head,L}$, TC$_{head,R}$, TC$_{tail,L}$, TC$_{tail,R}$) installed on the lifting buoys with the far ends of the lines anchored to seafloor at two sides of the system, as shown in Fig. 1. Pulling or relaxing the lateral control lines moves the lifting buoys laterally toward the left or the right of the tidal stream.

Being able to adjust the angle of deployment of the array tether means the ability to adjust spacing and relative positions of turbine units. This enables turbines formation adjustment (1D array or 2D formation) in response to flow pattern variations to achieve best formation efficiency. Further, large displacements of turbine arrays can accommodate deviations of tidal stream core passages.

III. Design and Feasibility Analysis

An example turbine design was made to study the design details and the feasibility of the proposed mooring concept. The assumed site of operation is in the Penghu Channel, west of Taiwan, along 50-100 m deep offshore area where maximal tidal flood speed can approach or exceed 2.5 m/s, under the additional effect from the Kuroshio branch current [11, 13]. Rotor radius R of the example turbine was set to 10 m; operational flow speed V_0 range 1-3 m/s. Basic thrust D_t, torque M_r and power P_t data can be estimated by the following relations:

Power available for capture is

$$P_t = C_p \pi R^2 \frac{\rho V_o^3}{2} \quad (1),$$

which relates to torque and rotational speed ω_t as

$$P_t = M_r \omega_t \quad (2),$$

$$\omega_t = \frac{\lambda V_o}{R} \quad (3).$$

The above equations lead to expression of torque as

$$M_r = \frac{C_p \pi R^3}{\lambda} \frac{\rho V_o^2}{2} \quad (4).$$

And the thrust is

$$D_t = C_{Dt} \pi R^2 \frac{\rho V_o^2}{2} \quad (5).$$

Assuming a thrust coefficient C_{Dt} = 0.89 (the ideal Betz situation, as the worst scenario), rotor tip speed ratio λ = 5 and a power coefficient C_p = 0.5, the estimated basic data are shown in Tab. I.

TABLE I
BASIC POWER, THRUST AND TORQUE ESTIMATIONS OF THE EXAMPLE TURBINE

Flow speed V_0 (m/s)	**Power** P_t (kW)	**Thrust** D_t (ton)	**Torque** M_r (ton-m)
1.0	81	16.4	16.4
2.0	644	58.4	65.6
3.0	2,174	132.0	148.0

A. Single turbine mooring and torque balancing

From Fig. 2(b), force balance gives the tensions and the angle of the of mooring lines in relation to the turbine thrust, turbine buoyancy B_t and turbine air weight W_{tn},

$$D_t = (T_{my,L} + T_{my,R}) = (T_{m,L} + T_{m,R}) \cos\theta_m \quad (6).$$

$$B_t = W_{tn} + (T_{mz,L} + T_{mz,R}) = W_{tn} + (T_{m,L} + T_{m,R}) \sin\theta_m \quad (7).$$

The locations of the buoyancy center and the mass center can be determined from

$$B_t(ab) >= W_{tn}(ac) \quad (8).$$

The torque from the rotor creates a difference in the tensions of the two mooring lines, which counter balances the torque, i.e.,

$$M_r = (T_{mz,L} - T_{mz,R}) s_{mh} \quad (9).$$

Regarding the design of the mooring base, Figure 5 shows a force analysis on the mooring base. The seagull shaped frame

places both ballasts (W_b) at the same elevation at 45° relative to the center of rotation o (the array tether) when there is no turbine torque exerted on the base. When the base rotates by an angle θ_b, a change of potential energy of the two ballasts creates a recovery torque, as

$$M_{bm} = W_b \frac{s_{bm}}{\sqrt{2}} \left[\sin\left(\frac{\pi}{4} + \theta_b\right) - \sin\left(\frac{\pi}{4} - \theta_b\right)\right] \quad (10).$$

s_{bm} is the span of the two ballasts. The 45° angle was found to provide maximal recovery torque at a given rotational angle. This recovery torque M_{bm} should be made larger than M_r.

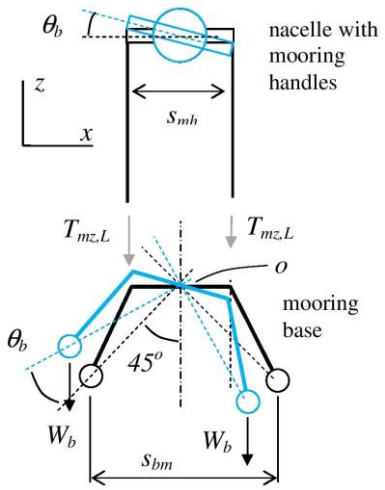

Fig. 5 Mooring base design force analysis.

By setting and adjusting total buoyancy B_t, turbine air weight W_{tn}, locations of buoyancy center and mass center ab and ac, mooring handle span d and mooring base ballasts span s_{bm}, an example mooring design was obtained. See Tab. II and Tab. III.

TABLE III
EXAMPLE TURBINE MOORING DESIGN PARAMETERS

Turbine buoyancy B_t (ton)	115.0
Turbine mass W_{tn} (ton)	38.0
ab (m)	0.31
ac (m)	5.0
Mooring handles span s_{mh} (m)	6.0
Base ballasts span s_{bm} (m)	12.0

TABLE IIIII
ESTIMATED MOORING TENSIONS, MOORING ANGLE AND ROLL ANGLE OF THE EXAMPLE TURBINE MOORING DESIGN PER TAB. II

Flow speed V_0 (m/s)	**Tensions L** $T_{m,L}$ (ton)	**R** $T_{m,R}$ (ton)	**Mooring angle** θ_m (degree)	**Roll angle** θ_b (degree)
1.0	39.6	36.9	79.2	2.1
2.0	43.7	32.8	52.6	8.4
3.0	50.6	26.0	30.2	19.0

A few limiting factors were considered in this example design. First, there is a practical range of turbine mass, considering masses of generators, gearbox and rotors of systems of similar power capacity. Second, the nacelle diameter should have a limit for not affecting the flow entering the rotor too much. The results in Tab. II give a nacelle dimension at about 2.5 m diameter by 25 m long. Third, the mooring angle under fast flow should be large enough so that the vertical force components are large enough to counter turbine torque. And finally, the roll angle should not be too large.

B. Turbine array depth keeping

By matching the designs of the mooring system of the turbine unit, the end clumps systems at both ends of the array tether and the lifting buoys, the turbines can be kept within a preferred depth range in most conditions.

Referring to Fig. 4(a), the depth of the turbine units is

$$d_{TU} = d_{LBF} + d_{LM} - d_{TM} \quad (11).$$

d_{TM} is the vertical distance between the turbines and their mooring bases on the array tether and can be determined from the mooring angle θ_m and length of turbine mooring lines. d_{LM} is the vertical distance between the lifting buoy fairlead (LBF_{head}) and the array tether and can be determined from length L_{hh} and angle θ_f of the hanging section by

$$d_{LM} = L_{hh} \sin \theta_f \quad (12).$$

The angle θ_f can be determined by

$$W_{ca} = T_a \tan \theta_f \quad (13),$$

wherein W_{ca} is weight of the end clump and T_a is the total tension exerted by the array of turbines, referring to Fig. 4(b). In other words, for a given array of turbines, adjusting W_{ca} and L_{hh} can change d_{LM}. And finally, the depth of the lifting buoy fairlead d_{LBF} depends on the structure of the main mooring tether (TM_{head}) and the net buoyancy of the lifting buoy B_{LBF}.

Also take note that when the whole turbine array is kept near-neutral buoyancy, vertical downward pull W_{ca} from the end clump and horizontal pull T_a from the array tether transmit to the lifting buoy fairlead directly and affect d_{LBF} as well. But the effect of W_{ca} can be removed by include it into the design of the lifting buoy B_{LBF}. The shape of the main mooring tether and d_{LBF} can be simulated by a 2D finite element model.

TABLE IVV
EXAMPLE MOORING SYSTEM DESIGN

Turbines mooring	
turbine mooring line length L_{tm} (m)	20
Array tether	
number of example turbines in array	8
hanging section length L_{hh} (m)	36
end clump net weight W_{ca} (ton)	100
inter-turbine distance (m)	100
array tether length (m)	900
no-flow tether tension (ton)	20
Main mooring tether	
main mooring tether length (m)	800
number of main tether buoys	10
Target hub (nacelle) depth (m)	30

Combining the above relations, an example end clump system and main tether design were made. Table IV lists major design parameters.

Fig. 6(a) shows estimated depths of turbines in the operating flow speed range when the above depth keeping method is applied, in comparison with the situation when no correction mechanism is used, and with other parameters. Fig. 6(b) shows the corresponding lifting buoy design, the buoyancy to depth relation, to achieve the depth keeping with the mechanism. The turbine can be maintained within a few meters around the target depth 30 m within the operating flow speed range.

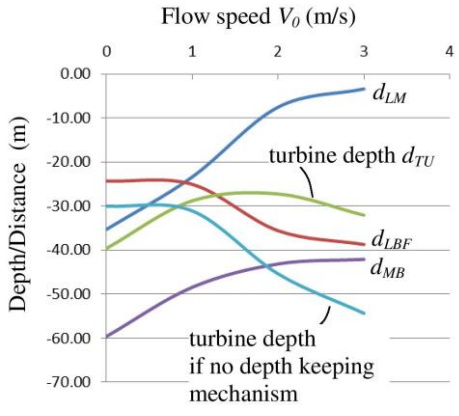

(a)

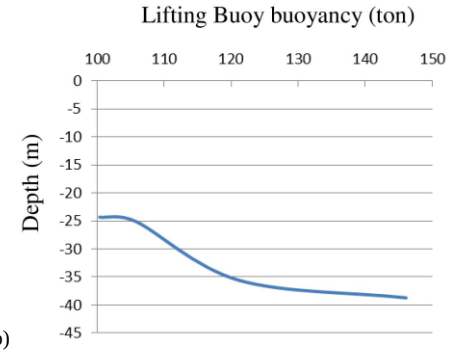

(b)

Fig. 6 (a) Estimated turbine depths in different flow speeds when the depth maintaining mechanism is applied, in comparison with the situation when no correction mechanism is used. d_{MB} is depth of the mooring bases on the array tether. d_{LM} and d_{LBF} see Fig. 4(a) and texts. (b) Buoyancy to depth relation of the corresponding lifting buoy design.

C. Turbine array deployment and bidirectional operations

Figure 7 illustrates a top view of a generalized 2D layout of the array tether when deployed across stream, with force diagrams at nodes. The array tether has N sections with N+1 nodes. Node N+1 is the head node and node 0 is the tail node. N turbine units are attached respectively to nodes 1 to N. All forces shown are on horizontal plane (x-y plane). Each turbine unit is subjected to a drag (thrust) force D_t. In this approximate analysis, drags over the tether and parts other than the turbines are neglected because of their small frontal areas compared to the turbine rotor sweep areas. As a result, at peak flow, a force of ND_t in the –y-direction is needed at the head node to hold the turbine array. To deploy the turbine array across the tidal stream, a lateral control force F_{lc} is applied to node 0 in x-direction. Balance of tension $T_{a,n}$ in each tether section with external forces on each node (n= 0, 1, … N) in x- and y- directions can then be written as

$$T_{a,n}\cos\theta_{a,n} = F_{lc} \quad (15)$$

and

$$T_{a,n}\sin\theta_{a,n} = nD_t \quad (16),$$

which lead to the deployment angle $\theta_{a,n}$ of each tether section as

$$\tan\theta_{a,n} = \frac{nD_t}{F_{lc}} \quad (17).$$

For $n = N$,

$$\tan\theta_{a,N} = \frac{ND_t}{F_{lc}} \quad (18).$$

Combining eqns. (17) and (18) gives

$$\tan\theta_{a,n} = \frac{n}{N}\tan\theta_{a,N} \quad (19).$$

Thus, total thrust (drag) in the turbine array and the lateral control force F_{lc} determines the deployment angle $\theta_{a,N}$ of the leading section of the array tether by eqn. (18). And eqn. (19) determines deployment angles of other sections relative to $\theta_{a,N}$. From the above relations, it is interesting to note that, during operation in flood tide or in ebb tide, if the ratio of D_t to F_{lc} is kept unchanged then the 2D layout of the turbine array will not change. This can be achieved by designing the main mooring tethers and arranging the tow lines at both sides of the system such that they are in tension and their lengths (spans) do not vary significantly within operating flow speed range. This way, by geometric similarity, D_t and F_{lc} will change in proportion and keep $\theta_{a,N}$ roughly constant.

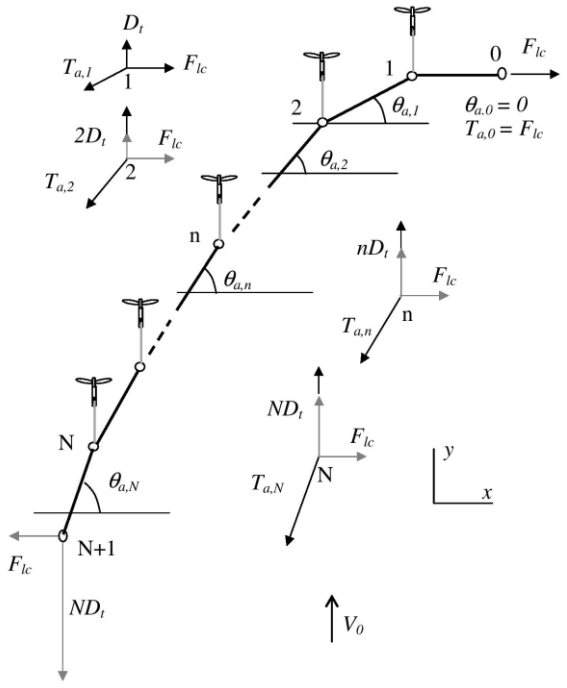

Fig. 7 Generalized 2D layout of a turbine array when deployed across stream, with force analysis.

Figure 8 shows examples of 2D layout of a turbine array of the design of Tab. IV under different conditions as estimated by the above relations. When there is no flow, the array is pulled straight (curve A) by the two end clumps and moored at two ends (A_h and A_t). When flood flow starts (toward y+ direction), the head end (A_h) is allowed to move until the main mooring tether's pull balances turbine thrusts but the tail end (A_t) does not move, thereby the array is pushed downstream to take a curve shape. For example, curve B_f corresponds to $\theta_{a,N}$ = 80° or $8D_t/F_{lc}$ = 5.67. When flood flow slows down and stop, the two end clumps pull the turbine array back to straight form (curve A). Then, when the reversed flow starts, the situation reverses and the turbine array is pushed to the opposite direction (curve B_e).

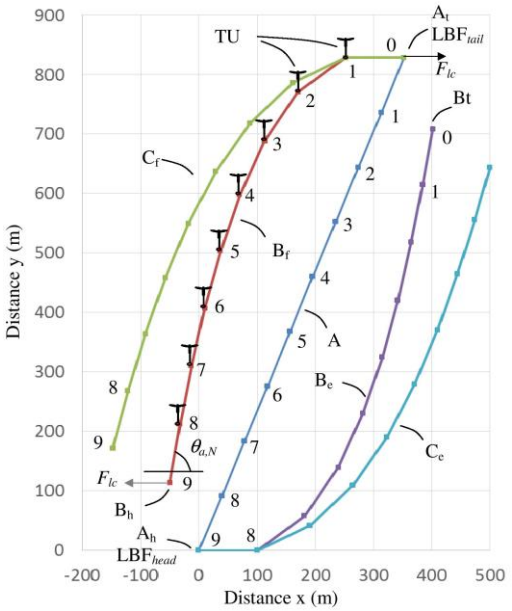

Fig. 8 Examples of 2D layout of a turbine array of the design of Tab. IV under different conditions.

From no-flow condition to operating conditions, the upstream end of the array is pulled downstream, e.g. from A_h to B_h in flood flow, by thrusts of the turbines so that the 2D curve of the array can form. Therefore, the main mooring tethers need a configuration that can provide this displacement. As shown in Fig. 1, buoys B_{tm} at equal distance along the main mooring tether suspend it in submerged floating so that catenary forms between adjacent buoys. The changes of the horizontal pull (from the turbine array) and the vertical force (buoyancy from the lifting buoy (LB_{head} or LB_{tail})) exerted at the fairlead (LBF_{head} or LBF_{tail}) change the total span of the main mooring tether, providing the needed displacement.

Figure 10 shows shapes of the example mooring tether of the design of Tab. IV when the turbine array is under different flow speeds, as computed by a basic finite element model. The total span of the mooring tether increases significantly from no-flow condition to operating conditions, providing the required displacement, but does not vary significantly within operating flow speed range, allowing the 2D layout of the turbine array to be kept unchanged.

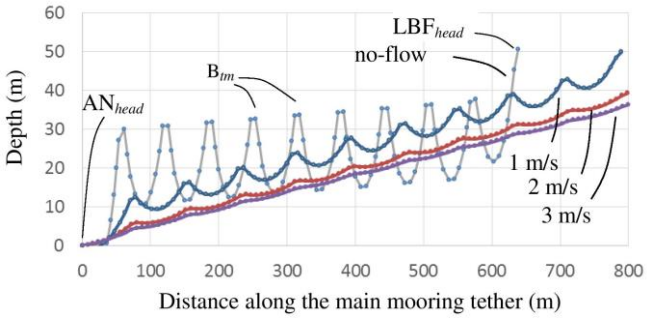

Fig. 9 Shapes of the example mooring tether of the design of Tab. IV when the 8-turbine array is under different flow speeds, as computed by a basic finite element model. Horizontal pulls were based on Tab. I. Vertical forces and fairlead depths correspond to data shown in Fig. 6.

D. Formations and Adjustments

Pulling or relaxing the lateral control lines moves the lifting buoys laterally toward the left or the right of the tidal stream. For example, in Fig. 8, shortening lateral control lines to the left of the turbine array increases F_{lc} and widens the spread of the layout, moving the turbine array from curve B_f to C_f, which corresponds to $\theta_{a,N}$ = 76.7° (or $8D_t/F_{lc}$ = 3.69).

Referring to Tab. I, within the 1-3 m/s operating flow speed range, total thrust $8D_t$ varies from 131 ton to 1056 ton. For layout B_f, the corresponding lateral force F_{lc} varies from 23.1 to 186 ton. For layout C_f, F_{lc} varies from 35.6 to 286 ton.

Adjustment of array layout should be performed during no or low flow period so that the winches only need to deal with low flow drag over the system.

E. Tethers and Power takeoff

Galvanized marine wire ropes are cost effective to be used to construct the tethers and the lateral control lines of the proposed system.

Power transmission cables from turbine units are first routed down to the mooring bases (Fig. 2(a)) and then placed along the array tether (CE, Fig. 1) and the main mooring tether to a position close to the main anchor (AN_{head}). From there, the cable is connected to shore.

IV. Model Tests: Preliminary Results

Scaled models were made and tested in a recirculating water tank to show the feasibility of the proposed mooring methods. To match the size of the small water tank, the model was made at 1/250 scale by Froude scaling. Table V shows the modelling parameters used. The turbine nacelle was made from foam board and the rotor disk was made from plastic sheet, so that the mass scale can be satisfied. The rotor was modelled by a fixed disk with cut partial openings and folds to provide thrust and torque simultaneously. Froude scaled thrust and torque of the model disk use full scale values in 2 m/s flow as targets, referring to Tab. I. The mooring base was made from plastic sheets and steel bolts.

Figure 10 shows the model in the water tank under a flow of ~12 cm/s (~2 m/s full scale). The shape of the rotor disk and the structure of the mooring base can be seen. The mooring base sit on a thin rope modelling the array tether. The

single turbine rode the flow in horizontal pose without rolling, demonstrating the torque countering function of the mooring base.

TABLE V
MODEL TURBINE MOORING TEST PARAMETERS

	1/250 x model	Full scale
Nacelle length	100 mm	25 m
Nacelle diam.	10 mm	2.5 m
Total air mass	2.28 g	35.6 ton
Total immersion buoyancy	7.28	113.6 ton
Rotor thrust ~12 cm/s (~2 m/s)	3.9 gw	60.8 ton
Rotor torque ~12 cm/s (~2 m/s)	1.8 gw-cm	70.2 ton-m
Mooring handles span	24 mm	6.0 m
Mooring base net weight	6.66 g	104 ton
Mooring base ballasts span	30 mm	7.5 m

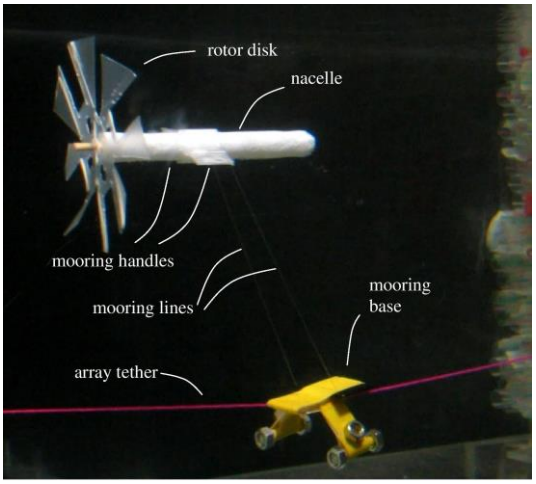

Fig.10 Close view of a model in the water tank under a flow of ~12 cm/s (~2 m/s full scale).

Figures 11 shows tests of an end clump system model for maintaining turbine depth. Due to the size of the water tank, only one turbine model was tested. Also, the tether's hanging section was fixed to tank walls. Fig. 11(a) shows the setup the end clump model. A depth marker on the flow regulator was used as a reference for observing depth change. In this no flow condition, the turbine model floated up vertically. Fig. 11(b) shows the situation in a flow of ~6 cm/s (1 m/s). It can be seen that at this lower end of operating speed, the turbine model can rotate to horizontal pose. Fig. 11(c) and 11(d) show the situations in flows of ~12 cm/s (2 m/s) and ~18 cm/s (3 m/s) respectively. In Fig. 11(d), it can be seen that the head clump is being pulled upwards. The depth of the turbine is generally maintained at the same level. In all cases, the model maintained horizontal pose without rolling.

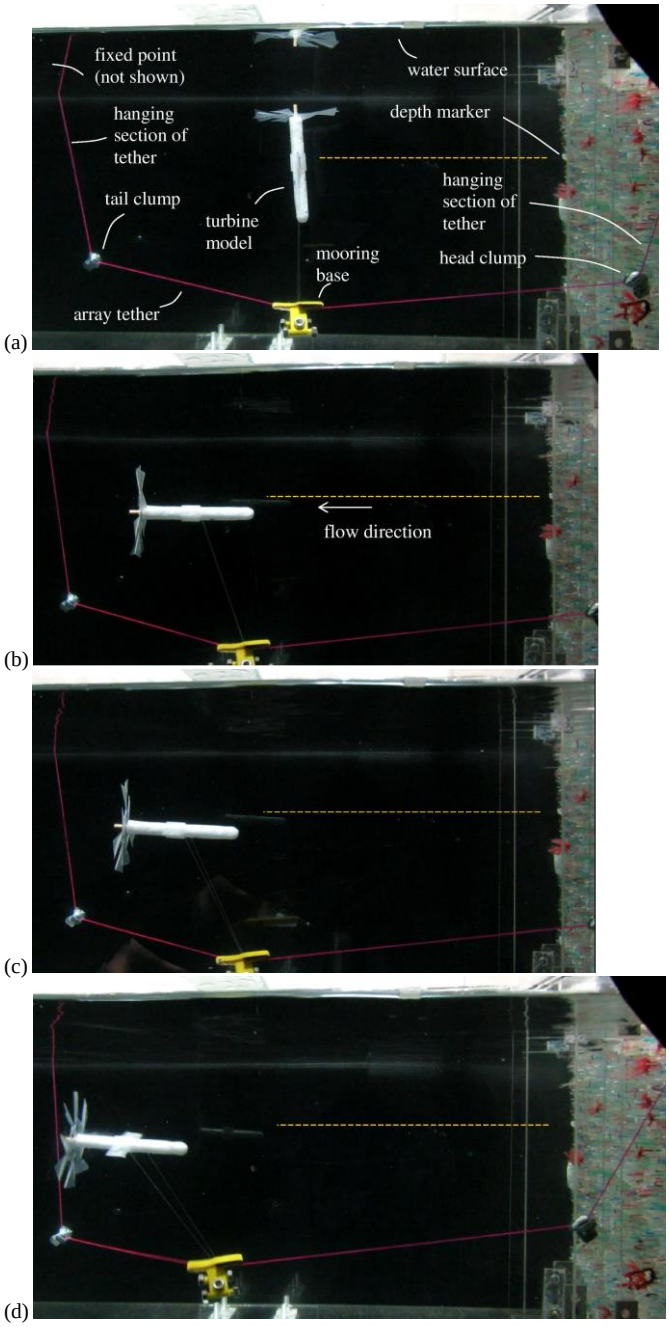

Fig. 11 Model tests of an end clump system for maintaining turbine depth; (a) no flow, (b) flow speed ~6 cm/s (~1m/s), (c) ~12 cm/s (~2 m/s), (d) ~18 cm/s (~3 m/s).

V. CONCLUSIONS AND FUTURE WORKS

A new design for mooring tidal stream turbines is proposed and its feasibility is studied by analysis and scaled model tests. The design features mooring multiple turbines on a common tether with anchoring only at two ends. The whole array of turbines is in submerged floating with only two major lifting buoys partially over water surface. Each turbine unit is moored to the common array tether by a system of dual mooring lines with mooring handles on the turbine and a mooring base on the array tether. The mooring system is able

to moor a single turbine, prevent it from rolling and also allow bi-directional operation by a vertical flipping motion. An end clump system was also designed to work with individual turbine mooring and the lifting buoys to maintain the turbines within a depth range in varying operational flow speeds.

Analysis in mechanics provided example designs and corresponding parameters. Scaled model tests demonstrated the feasibility of the single turbine mooring method and the end clump depth maintaining approach.

This design requires only very limited marine construction works, reducing installation costs and minimizing environmental impacts. It enables usage of most sea surface areas in a site by maintaining the turbines within a prescribed depth range regardless of depth of seafloor. It can place turbines closely while avoiding the risk of mechanical interference, because of the use of the common array tether. The single turbine mooring method can simplify configuration of the turbine. In addition, the design allows the application of lateral control lines to adjust array formation in response to flow pattern variations to achieve best formation efficiency. Further, large lateral displacements of turbine arrays can accommodate deviations of core passages of tidal flows.

Future works are under planning to study and to experimentally test model turbine arrays in a pool with simulated flows.

ACKNOWLEDGMENT

The current research is partially funded by the Ministry of Science and Technology of the R.O.C. under project number MOST 106-2221-E-007-100.

REFERENCES

[1] S. J. Sangiuliano, "Turning of the tides: Assessing the international implementation of tidal current turbines," *Renewable and Sustainable Energy Reviews*, vol. 80, pp. 971–989, 2017.

[2] E. Rolling, "MeyGen Tidal Energy Project EIA Scoping Document", accessed May 2018 from http://www.gov.scot/resource/0043/00434044.pdf

[3] Open Hydro Group., information from company website, see http://www.openhydro.com/ (Accessed May 2018)

[4] Scotrenewables Tidal Power Ltd., information from company website, accessed May 2018 from http://www.scotrenewables.com/technology-development/the-concept

[5] Bluewater Energy Services, "BlueTEC Texel Prototype," accessed May 2018 from http://www.bluewater.com/new-energy/texel-project/

[6] Black Rock Tidal Power, information from company website, accessed May 2018 from http://www.blackrocktidalpower.com/home/

[7] K. Shirasawa, K. Tokunaga, H. Iwashita and T. Shintake, "Experimental verification of a floating ocean current turbine with a single rotor for use in Kuroshio currents", *Renewable Energy*, vol. 91, pp. 189-195, 2016.

[8] Anonymous, "Power Generation Using the Kuroshio Current: Development of floating ocean current turbine system", *IHI Engineering Review*, Vol. 46, No. 2, 2014. Accessed July 2016 online: https://www.ihi.co.jp/var/ezwebin_site/storage/original/application/149ee9de3149aba2e1215fd5f9cd46ec.pdf

[9] L.-E. Myers and A.-S. Bahaj, "An experimental investigation simulating flow effects in first generation marine current energy converter arrays", *Renewable Energy*, vol. 37, pp. 28-36, 2012

[10] P. Stansby and T. Stallard, "Fast optimization of tidal stream turbine positions for power generation in small arrays with low blockage based on superposition of self-similar far-wake velocity deficit profiles," *Renewable Energy*, vol. 92, pp. 366-375, 2016

[11] Y.-H. Wang, L.-Y.Chiao, K.M.M. Lwiza and D.-P. Wang, "Analysis of flow at the gate of Taiwan Strait", *Journal of Geophysical Research*, vol. 109, C02025, 2004

[12] Y.-C. Chang, "Flow Observation in the Taiwan Strait and Adjacent Seas" (in Chinese with English summarizing paper manuscript), Ph.D. Thesis, National Sun Yat-Sen University, January 2008

[13] S.-F. Lin, C.-K. Hu and C.-W Yen, "The Estimation of ocean current power around Peng-hu," (in Chinese with English abstract) *Proceedings of the 33rd Ocean Engineering Conference in Taiwan*, National Kaohsiung Marine University, Dec. 2011, pp. 871

[14] L. Goddijn-Murphy, D.K. Woolf and M.C. Easton, "Current patterns in the Inner Sound (Pentland Firth) from underway ADCP data," *Journal of atmospheric and oceanic technology*, vol. 30, pp. 96-111, 2013

[15] P. Garcia Novo, "Study on ocean turbulence intensity around the Goto Island by field observation and numerical simulation," Kyushu University, Jul. 2016. From https://catalog.lib.kyushu-u.ac.jp/opac_detail_md/?lang=0&amode=MD823&bibid=1785433

[16] H.-W. Qin, Z. Cai, H.-W. Zhou, H.-M. Hu, "Three-dimensional numerical simulation of Zhoushan area," (in Chinese with English abstract) *Journal of Mechanical & Electrical Engineering*, vol. 31, no. 4, Apr. 2014, pp. 541-544

[17] L.-Y. Chang, F. Chen and K.-T. Tseng, "Dynamics of a marine turbine for deep ocean currents", *Journal of Marine Science and Engineering*, 4, 59, 2016

[18] C.-C. Tsao, A.-H. Feng, C. Hsieh and K.-H. Fan, "Marine Current Power with Cross-stream Active Mooring: Part I", *Renewable Energy*, vol. 109, pp. 144-154, 2017.

[19] C.-C. Tsao, L. Han, W.-T. Jian, C.-C. Lee, J.-S. Lee, A.-H. Feng, C. Hsieh, "Marine Current Power with Cross-stream Active Mooring: Part II", *Renewable Energy*, vol. 127, pp. 1036-1051, 2018.

[20] C.-C. Tsao and A.-H. Feng, "Motion Model and Speed Control of the Cross-stream Active Mooring System for Tracking Short-term Meandering to Maximize Current Power Generation", *Journal of Mechanics*, published online Dec. 4th, 2017.

[21] J. Twele, C. Heilmann and M. Schubert, "Wind turbines – design and components", Chap. 3 of *Wind power plants: Fundamentals, Design, Construction and Operation*, ed. by Gasch, R. and Twele, J. Berlin, Springer-Verlag, 2012.